

COMPACT OCT ENDOMICROSCOPIC CATHETER USING FLIP-CHIP BONDED LISSAJOUS SCANNED ELECTROTHERMAL MEMS FIBER SCANNER

Yeong-Hyeon Seo, Kyungmin Hwang, and Ki-Hun Jeong*

Department of Bio and Brain Engineering, KAIST, Daejeon, Republic of Korea

ABSTRACT

We report a compact optical coherence tomography (OCT) endomicroscope with a Lissajous scanned electrothermal MEMS fiber scanner. Two-dimensional Lissajous scanning was realized by Joule heating of the electrothermal MEMS fiber scanner. The compact packaging of MEMS scanner has a primary challenge, particularly in inserting it into an endomicroscopic catheter. The electrothermal MEMS fiber scanner was precisely designed and flip-chip bonded with a thin printed circuit board and completely packaged with 1.65 mm diameter housing tube, 1 mm diameter GRIN lens, and a single mode optical fiber. A 1.65 mm diameter OCT endomicroscopic catheter was successfully combined with a spectral-domain OCT system. Two-dimensional OCT image of a finger nail was successfully obtained with the endomicroscopic catheter.

KEYWORDS

MEMS fiber scanner, Endoscopic catheter, Endomicroscopy, Flip-chip, MEMS packaging, Lissajous laser scanning, Electrothermal MEMS actuator

INTRODUCTION

Optical endomicroscopy such as optical coherence tomography (OCT) [1-3], confocal [4], multi-photon imaging [5] has been demonstrated as a powerful imaging tool for in-vivo diagnosis such as optical biopsy [6, 7]. Especially, OCT imaging has a great potential for clinical diagnosis, such as, cancer screening with high resolution and cross-sectional imaging [1-3, 7-11]. A miniaturized forward-viewing endomicroscopic catheter provides a new clinical trial and diagnosis through the accessory channel of endoscope. Integration of high-resolution optical imaging into a small diameter probe provide non-invasive and real-time diagnosis of suspected lesions.

Resonant fiber scanner provides high scanning amplitude within low operating voltage, and it has been developed for OCT endomicroscopic applications. A quadratic piezoelectric tube (PZT) are widely applied for resonant fiber scanning actuators owing to some technical merits, such as compact and robust packaging [8-12]. Nevertheless, PZT fiber scanners still have some technical limitations in further miniaturization and lower cost.

Currently, micro-electro-mechanical system (MEMS) techniques provide a new breakthrough for miniaturized OCT endomicroscopic catheters. Small size, high speed, and low cost MEMS device enables optical scanning within restricted catheter space. Y.-H. Seo et al., have recently demonstrated Lissajous scanned electrothermal MEMS fiber scanner in Optical Express and IEEE MEMS 2016 [13, 14]. Electrothermal MEMS fiber scanner gives ultrathin dimensions and low cost price comparing with

conventional PZT fiber scanner. Moreover, MEMS fiber scanner provide Lissajous scanning, so that, the scanner provides uniform optical density and fast preview of an entire image area. Several endomicroscopic catheters using MEMS scanners such as electrostatic, electromagnetic, electrothermal actuation mechanisms have been demonstrated but they still have substantial problems in miniaturizing the endomicroscopic package due to electrical wiring or MEMS device mounting.

CONCEPT AND PRINCIPLE

We report the compact OCT endomicroscopic catheter using flip-chip bonded Lissajous scanned electrothermal MEMS fiber scanner (Fig. 1(a)).

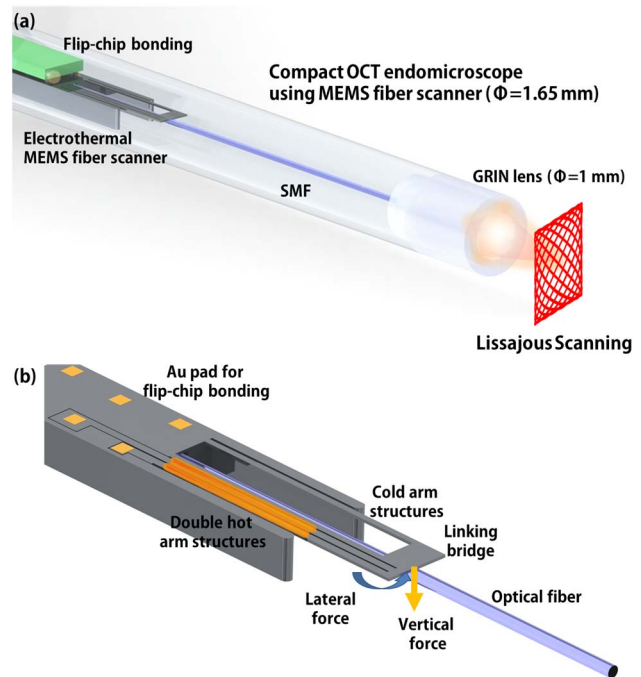


Figure 1: (a) Compact OCT endomicroscopic catheter with Lissajous scanned electrothermal MEMS fiber scanner. The MEMS fiber scanner was designed for flip-chip bonding, and integrated with printed-circuit board. MEMS fiber scanner was fully packaged with 1.65 mm diameter. (b) Working principle of the Lissajous scanned electrothermal MEMS fiber scanner. The scanner consists of double hot arm structure, cold arm structure, and a directly mounted optical fiber. Thermal expansion of hot arm structures induced by Joule heating enables lateral scanning, and bimorph structure between silicon cantilever of the scanner and mounted optical fiber induces vertical scanning. The asymmetric structure of microactuator differentiates the effective stiffness in both directions, and coupled static motion was completely removed in a resonant motion, which enables Lissajous scanning.

The MEMS fiber scanner consists of double hot arm structure and a directly mounted single mode optical fiber (Fig. 1(b)). Lateral motion is derived by thermal expansion of hot arm structures due to Joule heating and vertical motion is induced by bimorph structures by heated MEMS fiber scanner and mounted fiber. The asymmetric structure of microactuator differentiates the effective stiffness of optical fiber in both directions, and coupled static motion was completely removed in a resonant motion, which enables Lissajous scanning.

FABRICATION OF FLIP-CHIP BONDED MEMS FIBER SCANNER

The schematic of electrical packaging of the MEMS fiber scanner is described in Fig. 2(a). The compact packaging was achieved by using flip-chip bonding with six Au pads on the MEMS fiber scanner. The Au pads are patterned on the top silicon of the MEMS fiber scanner, i.e., 2 pads for actuation and 4 pads for stable flip-chip bonding. The 0.2 mm thick printed circuit board was simultaneously designed and flip-chip bonded with the MEMS fiber scanner. The inner diameter of the flip-chip bonded MEMS fiber scanner is only 1.3 mm and the fully packaged endoscopic catheter was precisely assembled with a 1.65 mm diameter stainless tube and 1 mm diameter GRIN lens. The microactuator is fabricated by using deep reactive ion etching (DRIE) on a heavily boron doped 6 inch silicon-on insulator (SOI) wafer (Top: 30 μm , BOX: 2 μm , Bottom: 400 μm), as shown Fig. 2(b). After microactuator fabrication, microactuator was released and assembled with single mode optical fiber with UV curable polymer (NOA 63).

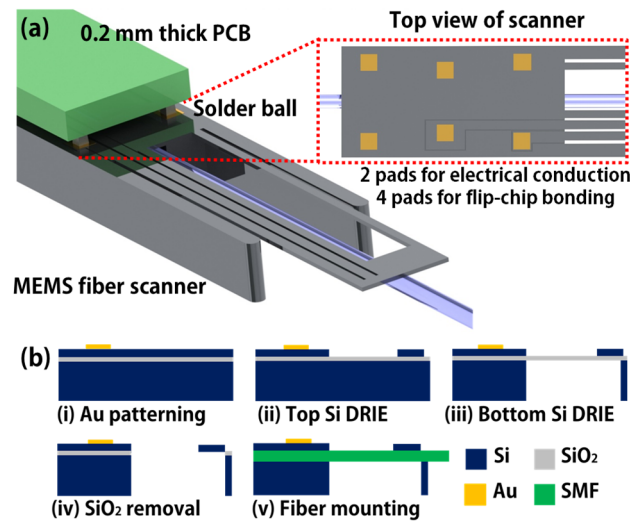


Figure 2: (a) Schematic of electrical packaging of the MEMS fiber scanner. The compact package was achieved by using flip-chip bonding with six Au pads on the MEMS fiber scanner. The Au pads are patterned on the top silicon of the MEMS fiber scanner, i.e., 2 pads for actuation and 4 pads for stable flip-chip bonding. The 0.2 mm thick printed circuit board was simultaneously designed and flip-chip bonded with the MEMS fiber scanner. (b) Microfabrication procedure for MEMS fiber scanner. The microactuator is fabricated by using deep reactive ion etching (DRIE) on a heavily boron doped 6 inch SOI wafer (Top: 30 μm , BOX: 2 μm , Bottom: 400 μm). After microactuator fabrication,

microactuator was released and assembled with single mode optical fiber with UV curable polymer (NOA 63).

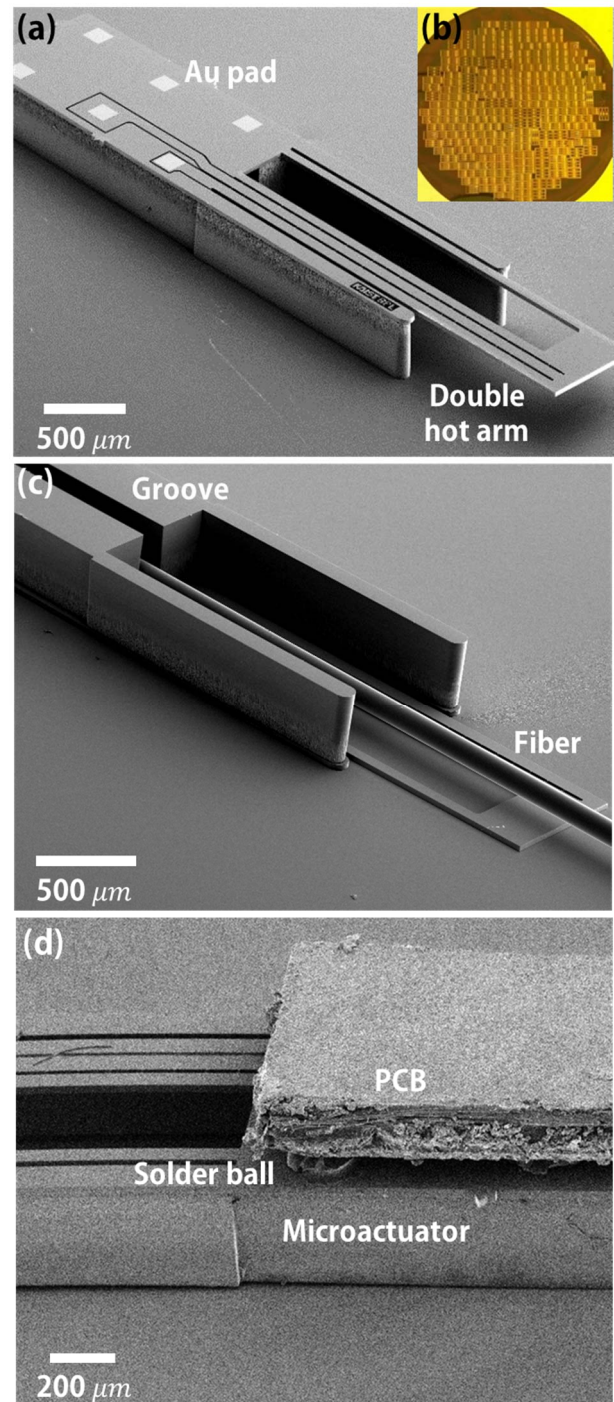


Figure 3: (a) Top SEM images of the microactuator. Double hot arm structures and 6 Au pad for flip-chip bonding are well defined. The footprint dimension of fabricated microactuator indicates $1 \times 5 \times 0.43 \text{ mm}^3$ (scale bar: 500 μm). (b) An optical image of the microfabricated 6 in. SOI wafer. Microactuators were well fabricated at a wafer level. (c) Bottom SEM image of microactuator (scale bar: 500 μm). 125 μm diameter single mode optical fiber is up on the fiber groove of the microactuator. (d) Side-view SEM images of the flip-chip mounted scanner (scale bar: 200 μm). 0.2 mm thick printed-circuit board is well attached to the microactuator with solder ball.

Figure 3(a) shows top SEM images of the microactuator. On the top side, 6 Au pads and double hot arm structures were well defined. The device footprint size indicates $1 \times 5 \times 0.43 \text{ mm}^3$. Microactuators were successfully fabricated at a wafer level, as shown Fig. 3(b). Figure 3(c) shows bottom SEM image of the microactuator. 125 μm single mode optical fiber is assembled to the microactuator. Figure 3(d) shows side SEM image of the flip-chip mounted scanner. 0.2 mm thick printed-circuit board is well attached to the microactuator with solder ball.

CATHETER PACKAGING AND OPTOMECHANICAL CHARACTERIZATION

Figure 4(a) shows flip-chip mounted MEMS fiber scanner and endoscopic catheter assembly parts. A 20 mm long optical fiber is attached to the flip-chip mounted MEMS fiber scanner. Figure 4(b) shows optical image of fully packaged OCT endoscopic catheter. Flip-chip design minimized electrical packaging dimension, so that, the inner diameter of the flip-chip bonded MEMS fiber scanner is only 1.3 mm, and OCT endoscopic catheter was precisely assembled with a 1.65 mm diameter stainless tube and 1 mm diameter GRIN lens.

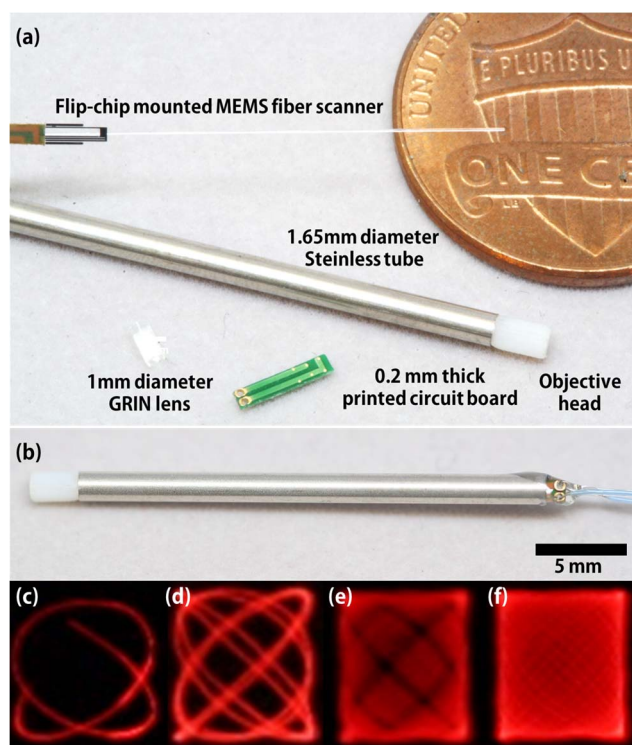


Figure 4: (a) Flip-chip mounted MEMS fiber scanner and endoscopic catheter assembly parts. A 20 mm long optical fiber is attached to the flip-chip mounted microactuator. (b) Fully packaged endoscopic catheter. The inner diameter of the flip-chip bonded MEMS fiber scanner is only 1.3 mm and the OCT endoscopic catheter was precisely assembled with a 1.65 mm diameter stainless tube and 1 mm diameter GRIN lens (scale bar : 5mm). (c)-(f) Lissajous patterns of electrothermal MEMS fiber scanner. $389 \mu\text{m} \times 452 \mu\text{m}$ field-of-view (F.O.V) Lissajous patterns was obtained within $16 V_{pp}$ operation voltage (scanning time: 1/125 sec, 1/40 sec, 1/10 sec, 1/4 sec).

Figure 4(c)-4(f) are time elapsed optical images of Lissajous patterns of electrothermal MEMS fiber scanner (scanning time: 1/125 sec, 1/40 sec, 1/10 sec, 1/4 sec). Rectangular pulse is applied to the MEMS fiber scanner for Lissajous scanning [13], and $389 \mu\text{m} \times 452 \mu\text{m}$ field-of-view (FOV) Lissajous patterns were successfully obtained within $16 V_{pp}$ operation voltage.

SPECTRAL-DOMAIN OCT IMAGING USING ENDOMICROSCOPIC CATHETER

Figure 5(a) shows spectral-domain OCT (SD-OCT) system diagram with the endoscopic catheter. The FPGA system was also implemented to achieve real-time 2D OCT imaging. Figure 5(b) shows two-dimensional SD-OCT image of finger. Compact OCT endoscopic catheter was successfully combined with SD-OCT system, and two-dimensional OCT images are successfully obtained within $16 V_{pp}$ operation voltage. This compact endoscopic catheter will give a new breakthrough to various endoscopic applications.

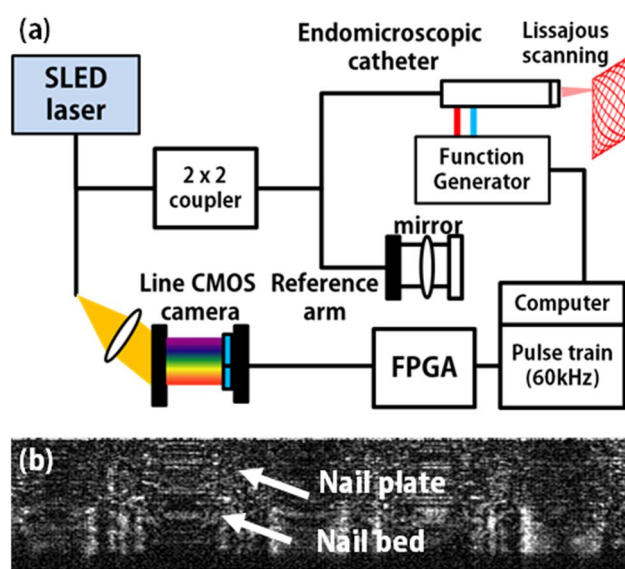


Figure 5: (a) Spectral-domain OCT system diagram with compact OCT endoscopic catheter. The FPGA system was also implemented to achieve real-time 2D OCT imaging. (b) Two-dimensional SD-OCT image of a finger nail. Two-dimensional OCT images are successfully obtained within $16 V_{pp}$ operation voltage.

CONCLUSION

To conclude, we have successfully demonstrated compact OCT endoscopic catheter using flip-chip bonded Lissajous scanner electrothermal MEMS fiber scanner. The electrothermal MEMS fiber scanner precisely designed for flip-chip bonding. The footprint dimension of fabricated microactuator indicates $1 \times 5 \times 0.43 \text{ mm}^3$. The compact packaging was achieved by using flip-chip bonding with six Au pads on the MEMS fiber scanner, i.e., 2 pads for actuation and 4 pads for stable flip-chip bonding. The inner diameter of the flip-chip bonded MEMS fiber scanner is only 1.3 mm, and OCT endoscopic catheter was precisely assembled with a 1.65 mm diameter

stainless housing tube and 1 mm diameter GRIN lens. 389 μm x 452 μm field-of-view (FOV) Lissajous patterns of were successfully obtained within 16 V_{pp} operation voltage using fabricated electrothermal MEMS fiber scanner. Compact OCT endomicroscopic catheter was successfully combined with spectral-domain OCT system, and two dimensional OCT image of a finger nail was obtained. 1.65 mm diameter OCT endomicroscopic catheter provides opportunities for various endomicroscopic applications with ultrathin and low cost.

ACKNOWLEDGEMENTS

This research was supported by a grant of the Korea Health Technology R&D Project through the Korea Health Industry Development Institute (KHIDI), funded by the Ministry of Health & Welfare, Republic of Korea. (grant number: HI13C2181, HI16C1111), the Ministry of Science, ICT and Future Planning (2016013061), and the Global Frontier Project (2016924609) of the Korea government.

REFERENCES

- [1] W. Hatta, K. Uno, T. Koike, K. Iijima, N. Asano, A. Imatani, et al., "A prospective comparative study of optical coherence tomography and EUS for tumor staging of superficial esophageal squamous cell carcinoma," *Gastrointestinal Endoscopy*, vol. 76, pp. 548-555, Sep 2012.
- [2] C. Duan, X. Zhang, D. Wang, Z. Zhou, P. Liang, A. Pozzi, et al., "An endoscopic forward-viewing OCT imaging probe based on a two-axis scanning mems mirror," in *Biomedical Imaging (ISBI), 2014 IEEE 11th International Symposium on*, 2014, pp. 1397-1400.
- [3] W. Jung, D. T. McCormick, Y.-C. Ahn, A. Sepehr, M. Brenner, B. Wong, et al., "In vivo three-dimensional spectral domain endoscopic optical coherence tomography using a microelectromechanical system mirror," *Opt. Lett.*, vol. 32, pp. 3239-3241, 2007.
- [4] T. Meinert, N. Weber, H. Zappe, and A. Seifert, "Varifocal MOEMS fiber scanner for confocal endomicroscopy," *Opt Express*, vol. 22, pp. 31529-31544, Dec 15 2014.
- [5] D. R. Rivera, C. M. Brown, D. G. Ouzounov, I. Pavlova, D. Kobat, W. W. Webb, et al., "Compact and flexible raster scanning multiphoton endoscope capable of imaging unstained tissue," *Proceedings of the National Academy of Sciences*, vol. 108, pp. 17598-17603, 2011.
- [6] B. J. Reid, P. L. Blount, Z. Feng, and D. S. Levine, "Optimizing endoscopic biopsy detection of early cancers in Barrett's high-grade dysplasia," *Am J Gastroenterol*, vol. 95, pp. 3089-3096, 11/print 2000.
- [7] B. J. Vakoc, D. Fukumura, R. K. Jain, and B. E. Bouma, "Cancer imaging by optical coherence tomography: preclinical progress and clinical potential," *Nat Rev Cancer*, vol. 12, pp. 363-368, 05/print 2012.
- [8] X. Liu, M. J. Cobb, Y. Chen, M. B. Kimmey, and X. Li, "Rapid-scanning forward-imaging miniature endoscope for real-time optical coherence tomography," *Opt. Lett.*, vol. 29, pp. 1763-1765, 2004.
- [9] H.-C. Park, Y.-H. Seo, and K.-H. Jeong, "Lissajous fiber scanning for forward viewing optical endomicroscopy using asymmetric stiffness modulation," *Opt Express*, vol. 22, pp. 5818-5825, 2014.
- [10] H.-C. Park, Y.-H. Seo, K. Hwang, J.-K. Lim, S. Z. Yoon, and K.-H. Jeong, "Micromachined tethered silicon oscillator for an endomicroscopic Lissajous fiber scanner," *Opt. Lett.*, vol. 39, pp. 6675-6678, 2014.
- [11] N. Zhang, T.-H. Tsai, O. O. Ahsen, K. Liang, H.-C. Lee, P. Xue, et al., "Compact piezoelectric transducer fiber scanning probe for optical coherence tomography," *Opt. Lett.*, vol. 39, pp. 186-188, 2014/01/15 2014.
- [12] K. Hwang, Y.-H. Seo, and K.-H. Jeong, "High resolution and high frame rate Lissajous scanning using MEMS fiber scanner," in *2016 International Conference on Optical MEMS and Nanophotonics (OMN)*, 2016, pp. 1-2.
- [13] Y.-H. Seo, K. Hwang, H.-C. Park, and K.-H. Jeong, "Electrothermal MEMS fiber scanner for optical endomicroscopy," *Opt Express*, vol. 24, pp. 3903-3909, 2016/02/22 2016.
- [14] Y. H. Seo, H. C. Park, and K. H. Jeong, "Electrothermal MEMS fiber scanner with lissajous patterns for endomicroscopic applications," in *2016 IEEE 29th International Conference on Micro Electro Mechanical Systems (MEMS)*, 2016, pp. 367-370.

CONTACT

*Ki-Hun Jeong, tel: +82-42-350-4323; kjeong@kaist.ac.kr